PHYSICAL REVIEW D **83,** 096006 (2011)

Covariant study of tensor mesons

A. Krassnigg* and M. Blank†

Institut für Physik, Karl-Franzens-Universität Graz, A-8010 Graz, Austria

(Received 3 December 2010; revised manuscript received 30 March 2011; published 16 May 2011)

We investigate tensor mesons as quark-antiquark bound states in a fully covariant Bethe-Salpeter equation. As a first concrete step we report results for masses of $J^{PC} = 2^{++}$ mesons from the chiral limit up to bottomonium and sketch a comparison to experimental data. All covariant structures of the fermion-antifermion system are taken into account and their roles and importance discussed in two different bases. We also review the general construction principle for covariant Bethe-Salpeter amplitudes of mesons with any spin.

DOI: 10.1103/PhysRevD.83.096006 PACS numbers: 11.10.St, 12.38.Lg, 14.40.−n

I. INTRODUCTION

In QCD, mesons are viewed as bound states of (anti) quarks and gluons. Starting with a $\bar{q}q$ picture they appear simpler than baryons and thus represent prime targets for theoretical investigations. Spin and the corresponding meson degrees of freedom are essential for an understanding of the meson spectrum and properties in general.

In a constituent-quark model (e.g., [1–6]), mesons with total spin J are easily obtained via adding units of orbital angular momentum to a quark-antiquark state. In particular, given the quantum numbers J^{PC} for a meson with equal-mass constituents, the parity P is given by $(-1)^{l+1}$ and the C parity C by $(-1)^{l+s}$. Furthermore, the total spin J, the internal (quark-antiquark) spin s, and the orbital angular momentum l and their projections have to satisfy the well-known addition rules for angular momenta.

In the context of the Bethe-Salpeter equation (BSE), the Lorentz covariant structure of meson amplitudes (also for arbitrary spin) has in the past been investigated mainly in setups involving reductions of the BSE (e.g., [7–20]). Herein we present the first covariant study of tensor mesons that is consistent with respect to the axial-vector Ward-Takahashi identity in the context of a Dyson-Schwinger–Bethe-Salpeter approach to QCD. This is a remarkable achievement due to the technical complexity of the problem and since such a study had not been attempted before despite the path laid out several decades ago [7].

The paper is organized as follows: Section II sketches the formalism used and the corresponding details of immediate necessity, Sec. III contains the explicit construction of the covariant amplitude for a 2^{++} meson, the construction principle for $J > 2$ amplitudes is reviewed in our notation in Sec. IV, the 2^{++} results are presented and discussed in Sec. V, and we conclude in Sec. VI. All calculations have been performed in Euclidean momentum space.

*andreas.krassnigg@uni-graz.at
†martina.blank@uni-graz.at

II. MESONS FROM THE BSE

In this work, we employ QCD's Dyson-Schwinger-equations (DSEs) (see, e.g., [21,22] for recent reviews) together with the quark-antiquark BSE. The latter is the covariant bound-state equation for the study of mesons in this context [7]. An analogous covariant approach to baryons is possible in a quark-diquark picture (e.g., [23–25] and references therein) or a three-quark setup [26,27].

While the goal of a self-consistent solution of all DSEs can be held up in investigations of certain aspects of the theory (see, e.g., [28,29] and references therein), numerical hadron studies such as ours require employment of a truncation. For our first covariant look at tensor mesons we use the so-called rainbow-ladder (RL) truncation. It is both simple and offers the possibility for sophisticated model studies of QCD within the DSE-BSE context, since it satisfies the relevant (axial-vector and vector) Ward-Takahashi identities (see e.g., [13,14,30–38]).

At this point, a remark regarding corrections to RL truncation is in order. Even with a sophisticated choice one cannot guarantee that contributions from the scalar part of the quark-gluon vertex can be mimicked successfully by an effective interaction. On the contrary, RL studies of light axial-vector mesons (see e.g., [39] and references therein) indicate that these states are in general not well described in such a setup; their masses are substantially underestimated, although this effect depends on the particular choice of model parameters [39]. Since the comparison to experimental data for the light scalar mesons is more difficult, the reasonable conclusion has been that the scalar part of the quark-gluon vertex is important for the description of mesons interpreted as orbital excitations (e.g., P wave).

Notwithstanding this, the overall situation in the meson spectrum might not be so complicated. In fact, RL truncation is expected to be a better approximation to QCD for higher quark masses, and a corresponding effort has been recently made to construct a quark-mass dependent effective interaction to account for a diminishing influence of

the scalar part of the quark-gluon vertex as the quark mass increases [40,41].

In addition, meson studies beyond RL truncation have confirmed the large effects from correction terms, but at the same time shown the enormous numerical complexity of such an endeavor together with the uncertainty of how large even further corrections are. With this in mind, RL truncation with an effective interaction was our preferred choice for the present study despite the expectation that P-wave states are possibly badly described in the light-meson sector. As our results show, this expectation is not entirely justified *a posteriori*. For completeness we note that the two main directions of improvement beyond RL truncation come on the one hand from employing corrections to the bare quark-gluon vertex from the DSE of the full quark-gluon vertex, and on the other hand from construction valid for more general forms of the quark-gluon vertex. The literature regarding these two possibilities can be traced back from e.g., [42,43], respectively.

The axial-vector Ward-Takahashi identity is essential to see chiral symmetry and its dynamical breaking correctly realized in the model calculation from the very beginning. As the most prominent result, one satisfies Goldstone's theorem [35] and obtains a generalized Gell-Mann–Oakes–Renner relation valid for all pseudoscalar mesons and all current-quark masses [44,45]. We note that this relation can be checked numerically and is satisfied at the per-mill level in our calculations. This model approach to mesons in QCD is well established and has been successfully applied to many, in particular, pseudoscalar- and vector-, meson properties in recent years (see e.g., [22,39] for comprehensive bibliographies).

The general structure of the BSE for a meson with spin J, total $q\bar{q}$ momentum P and relative $q\bar{q}$ momentum k or q, respectively, is

$$\Gamma^{\mu\nu\cdots}(k;P) = \int_q^\Lambda K(k;q;P) S(q_+) \Gamma^{\mu\nu\cdots}(q;P) S(q_-), \quad (1)$$

where the semicolon separates four-vector arguments. $\Gamma^{\mu\nu\cdots}(k;P)$ is the Bethe-Salpeter amplitude (BSA) and has J open Lorentz indices $\mu\nu\ldots$. The dressed-quark propagator $S(p)$ is obtained from the quark DSE, the QCD gap equation. Since our focus here is the BSA, we refer the reader to [39,44,46] for more details on the quark DSE and to [47] for a description of our corresponding numerical solution method. In the BSE the quark and antiquark propagators depend on the (anti)quark momenta $q_+ = q + \eta P$ and $q_- = q - (1-\eta)P$, where $\eta \in [0,1]$ is a momentum partitioning parameter usually set to $1/2$ for systems of equal-mass constituents (which we do as well). $\int_q^\Lambda = \int^\Lambda d^4q/(2\pi)^4$ represents a translationally invariant regularization of the integral, with the regularization scale Λ [44].

The kernel K in the homogeneous, ladder-truncated $q\bar{q}$ BSE is essentially characterized by an effective interaction $\mathcal{G}(s)$, $s := (k-q)^2$. Following [39], an ansatz used extensively for many years [46] is employed here,

$$\frac{\mathcal{G}(s)}{s} = \frac{4\pi^2 D}{\omega^6} s e^{-(s/\omega)^2} + \frac{4\pi\gamma_m \pi \mathcal{F}(s)}{1/2 \ln[\tau + (1 + s/\Lambda_{\mathrm{QCD}}^2)^2]}. \quad (2)$$

This form provides the correct amount of dynamical chiral symmetry breaking as well as quark confinement via the absence of a Lehmann representation for the dressed quark propagator. Furthermore, it produces the correct perturbative limit, i.e., it preserves the one-loop renormalization group behavior of QCD for solutions of the quark DSE. As given in [46], $\mathcal{F}(s) = [1 - \exp(-s/[4m_t^2])]/s$, $m_t = 0.5$ GeV, $\tau = e^2 - 1$, $N_f = 4$, $\Lambda_{\mathrm{QCD}}^{N_f=4} = 0.234$ GeV, and $\gamma_m = 12/(33 - 2N_f)$. Note that the same effective interaction appears also in the corresponding rainbow-truncated quark DSE. This function, which mimics the behavior of the product of quark-gluon vertex and gluon propagator, is mainly phenomenologically motivated. While currently debated on principle grounds (e.g., [29,48]) the impact of its particular form in the far IR on meson masses is expected to be small (see also [49] for an exploratory study in this direction).

D and ω, in principle free parameters of the model interaction, can be used to investigate certain aspects of both the interaction and the bound states in the BSE. In particular one can interpret D as an overall strength and ω as an inverse effective range of the interaction (for more details and a thorough discussion of parameter dependence of the results see [39]), a notion first investigated in the study of radial meson excitations [45,50]. In the range $\omega \in [0.3, 0.5]$ GeV, the prescription $D \times \omega = \text{const}$ follows from fitting of the model parameters to ground-state properties [46] and defines a one-parameter model, which is the setup and range used in [39] and also here. With all ingredients specified, the BSE is solved numerically, a procedure well under control [51].

III. TENSOR-MESON BSA

The BSA $\Gamma^{\mu\nu\cdots}(q;P)$ of a meson as a bound state of a quark-antiquark pair depends on two four-vector variables: the total as well as the relative $q\bar{q}$ four-momenta P and q, respectively. They can be parameterized in terms of the Lorentz-invariant scalar products P^2, q^2, and $q \cdot P$. The fermion-antifermion spin properties are encoded in the 4×4 matrix structure of $\Gamma^{\mu\nu\cdots}$ [7], where the open Lorentz indices appear in connection with the total spin of the state. A corresponding basis of linearly independent structures $\{T_i^{\mu\nu\cdots}\}$ $(i = 1, \ldots, N)$ involving Dirac matrices allows one to expand the BSA into a sum of Dirac covariants and the corresponding scalar coefficients F_i, which we will subsequently refer to as *components* [51]. The latter only depend on the aforementioned scalar products P^2, q^2, and $q \cdot P$, and one gets

$$\Gamma^{\mu\nu\cdots}(q;P;\gamma) = \sum_{i=1}^{N} T_i^{\mu\nu\cdots}(q;P;\gamma) F_i(q^2, q\cdot P, P^2), \quad (3)$$

where the dependence on γ^α has been made explicit and a generalized scalar product for the covariants $T_i^{\mu\nu\cdots}$ is defined via the Dirac trace

$$\sum_{\mu\nu\cdots} \mathrm{Tr}[T_i^{\mu\nu\cdots} T_j^{\mu\nu\cdots}] = t_{ij} f(i,j). \quad (4)$$

One may also choose the basis elements orthogonal such that $t_{ij} = \delta_{ij}$, with the $f(i,j)$ functions of q^2, P^2, and $q\cdot P$, or orthonormal such that in addition $f(i,j) = 1$ for all i, j. The sum is carried out over the J indices $\mu, \nu, \ldots$.

Note that for an on-shell BSA $P^2 = -M^2$ is fixed, while one artificially varies P^2 in the solution process of the homogeneous BSE. In the corresponding inhomogeneous BSE one has P and therefore also P^2 as a completely independent variable (see, e.g., [51–53]).

Thus, the on-shell scalar components $F_i(q^2, q\cdot P, P^2)$ effectively depend on the two variables q^2 and $q\cdot P$, the latter of which can be parameterized by the variable $z \in [-1,1]$ related to the cosine defining the angle between the four-vectors P and q. In principle, the components F_i can be expanded further in Chebyshev polynomials, but we do not use such an expansion here (for details and an illustration of Chebyshev moments, see [44,54]). With the independent four-momenta and γ^α one can construct four independent Lorentz-scalar structures,

$$\mathbf{1}, \qquad \gamma\cdot P, \qquad \gamma\cdot q, \qquad i\sigma^{q,P}, \quad (5)$$

where $\sigma^{q,P} := i/2[\gamma\cdot q, \gamma\cdot P]$. These four covariants, which provide a basis corresponding to scalar mesons ($J^P = 0^+$), serve as the basic building blocks for any meson BSA. Together with pseudoscalar covariants ($J^P = 0^-$) as well as the bases for $J = 1$ for all corresponding quantum numbers, these were explicitly constructed in [39]. Here we concentrate on $J = 2$ and higher.

For $J = 2$ one has eight independent covariant structures in the BSA. Let

$$q_\mu^T := q_\mu - P_\mu \frac{q\cdot P}{P^2}, \quad (6)$$

$$\gamma_\mu^T := \gamma_\mu - P_\mu \frac{\gamma\cdot P}{P^2}, \quad (7)$$

$$\gamma_\mu^{TT} := \gamma_\mu - P_\mu \frac{\gamma\cdot P}{P^2} - q_\mu^T \frac{\gamma\cdot q^T}{(q^T)^2} \quad (8)$$

be transverse projections of γ and q with respect to the total meson momentum P and each other (in particular the vectors $\{P_\mu, q_\mu^T, \gamma_\mu^{TT}\}$ are orthogonal to each other).

Defining furthermore the transverse projection of the metric

$$g_{\mu\nu}^T = \delta_{\mu\nu} - \frac{P_\mu P_\nu}{P^2} \quad (9)$$

and the two transverse, symmetric, and traceless structures

$$M_{\mu\nu} = \gamma_\mu^T q_\nu^T + q_\mu^T \gamma_\nu^T - \frac{2}{3} g_{\mu\nu}^T \gamma\cdot q^T \quad (10)$$

$$N_{\mu\nu} = \mathbf{1}\left(q_\mu^T q_\nu^T - \frac{1}{3} g_{\mu\nu}^T q\cdot q^T\right) \quad (11)$$

one obtains the following set of tensor ($J^P = 2^+$) covariants [7]:

$$\begin{aligned} T_1^{\mu\nu} &= iM^{\mu\nu} & T_2^{\mu\nu} &= M^{\mu\nu}\gamma\cdot q q\cdot P - 2N^{\mu\nu} q\cdot P \\ T_3^{\mu\nu} &= M^{\mu\nu}\gamma\cdot P & T_4^{\mu\nu} &= 2M^{\mu\nu}\sigma^{q,P} - 4iN^{\mu\nu}\gamma\cdot P \\ T_5^{\mu\nu} &= N^{\mu\nu} & T_6^{\mu\nu} &= iN^{\mu\nu}\gamma\cdot q \\ T_7^{\mu\nu} &= iN^{\mu\nu}\gamma\cdot P q\cdot P & T_8^{\mu\nu} &= -2iN^{\mu\nu}\sigma^{q,P} \end{aligned} \quad (12)$$

Note that $T_5 \ldots T_8$ were only given implicitly in [7]. All T_i as given here are even under charge conjugation (for details, see e.g., [39,44]). Thus, to obtain a $J^{PC} = 2^{++}$ state, all components F_i must be even functions of $q\cdot P$, which for the present setup is indeed the property of the ground state in the system. It is interesting to note at this point that all solutions reported here have positive canonical norm, since the BSE allows negative norm states and the appearance of spurious excitations in relative time (for an exploratory study of these issues and a possible connection between them, see e.g., [55] and references therein). Note also that the above covariants are in general neither orthogonal nor normalized; orthonormal covariants can be generated via a Gram-Schmidt procedure applied to the set of terms in (5), leading to

$$\mathbf{1}, \qquad \gamma\cdot P, \qquad \gamma\cdot q^T, \qquad i\sigma^{q,P}. \quad (13)$$

To orthogonalize the above 2^+ covariants one introduces the symmetric and transverse expressions

$$\tilde{M}_{\mu\nu} = \gamma_\mu^{TT} q_\nu^T + q_\mu^T \gamma_\nu^{TT} \quad \text{and} \quad (14)$$

$$\tilde{N}_{\mu\nu} = q_\mu^T q_\nu^T, \quad (15)$$

which automatically satisfy Eq. (4). The next step is to implement the tracelessness, which is equivalent to orthogonality with respect to $g_{\mu\nu}^T$. This yields

$$M_{\mu\nu} = \tilde{M}_{\mu\nu} - g_{\mu\nu}^T \frac{\tilde{M}_{\rho\sigma} g_{\rho\sigma}^T}{(g^T)^2} \quad (16)$$

$$N_{\mu\nu} = \tilde{N}_{\mu\nu} - g_{\mu\nu}^T \frac{\tilde{N}_{\rho\sigma} g_{\rho\sigma}^T}{(g^T)^2}, \quad (17)$$

which corresponds to Eqs. (10) and (11), and by multiplication with the four scalar covariants in (13) gives the eight desired orthogonal tensor covariants. Note, however, that Eqs. (10) and (16) are slightly different. Subsequently, normalization is achieved via $\hat{T}_i = T_i/\sqrt{\mathrm{Tr}[T_i\cdot T_i]}$.

IV. BSA FOR ANY MESON SPIN

To consider mesons of any particular spin J, one has to construct Lorentz tensors of rank J which are totally symmetric, transverse in all open indices and Lorentz traceless (see, e.g., [56]): such an object has the $2J + 1$ spin degrees of freedom as demanded in quantum mechanics of a massive particle. These restrictions, together with the properties of the Dirac matrices, lead to eight covariant structures for $J \geq 1$ [12,15]. More precisely, the two tensors $M_{\mu\nu}$ and $N_{\mu\nu}$ defined above can be generalized such that $N_{\mu\nu\ldots\tau}$ is the traceless part of

$$q^T_\mu q^T_\nu \ldots q^T_\tau \tag{18}$$

and $M_{\mu\nu\ldots\tau}$ is the traceless part of the totally symmetric sum constructed from

$$\gamma^{TT}_\mu q^T_\nu \ldots q^T_\tau. \tag{19}$$

Each of these multiplied by the four terms in (13) defines four rank-J tensor covariants, in total eight, orthogonal in the sense of Eq. (4).

Obviously, Eqs. (16) and (17) follow from this construction. As a further quick check we consider the simplest such example, namely, a vector meson: from $J = 1$ one immediately obtains $N_\mu = q^T_\mu$ to give the first four, and $M_\mu = \gamma^{TT}_\mu$ to give the second four covariants.

V. RESULTS AND DISCUSSION

Here we present results for $J^{PC} = 2^{++}$ states that extend the study of Ref. [39]. Consequently, we present correspondingly augmented figures here. Figure 1 shows the meson masses for pseudoscalar, scalar, vector, axial-vector, and tensor $q\bar{q}$ states as functions of the pion mass, obtained from the BSE in RL truncation employing the effective interaction of Eq. (2). The three vertical dotted lines indicate the positions of the $n\bar{n}$, $s\bar{s}$, and $c\bar{c}$ states, respectively, (in the usual notation, n here denotes light quarks). Note that in RL truncation one cannot easily employ arbitrary flavor mixing between $SU(3)$-flavor octet and singlet states; all states are either purely $n\bar{n}$ or $s\bar{s}$, which corresponds to *ideal* mixing. As expected, the 2^{++} mass lies above all other states for the entire range from the chiral limit to bottomonium. Furthermore, the quark model predicts [1] that the states with 0^{++}, 1^{++}, and 2^{++} are close together, consistent with experiment. While a similar pattern is realized also here for heavy quarks, the onset of which is visible in Fig. 1 and apparent from the rightmost column in Fig. 2, this is not the case for light mesons. The reason is that, in rainbow-ladder truncation with an effective interaction, the missing influence of the scalar part in the dressed quark-gluon vertex, which is essential for a good description of P-wave mesons, destroys the expected pattern of these $l = 1$ states for light quark masses. This is clearly the case for our results, where the corresponding splittings between 0^{++} and 1^{++} as well as 1^{++} and 2^{++} are too large.

However, the splittings of the 2^{++} states to the S-wave states is reproduced better, even for light mesons, and, in particular, if one takes the dependence of the meson masses on the model parameters into account. Comparison to experimental data is shown in Fig. 2 via the dotted lines in appropriate colors, where for the $n\bar{n}$, $s\bar{s}$, $c\bar{c}$, and $b\bar{b}$ cases separately the dependence of the bound-state masses on the model parameters is studied. More precisely, as mentioned in Sec. II, the inverse effective range ω is used to explore the state's sensitivity to the details of the long-range part of the strong interaction [39,45]. Two observations are

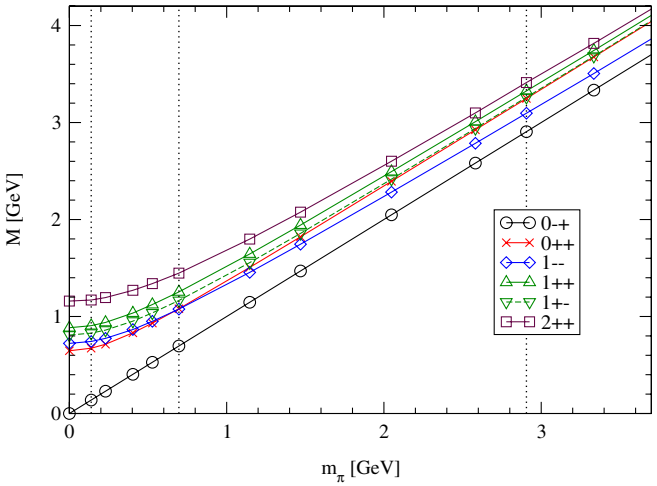

FIG. 1 (color online). Dependence of meson masses on m_π (the pseudoscalar-meson mass calculated for a given current-quark mass). Vertical dotted lines correspond to positions for light, strange, and charm $\bar{q}q$ states.

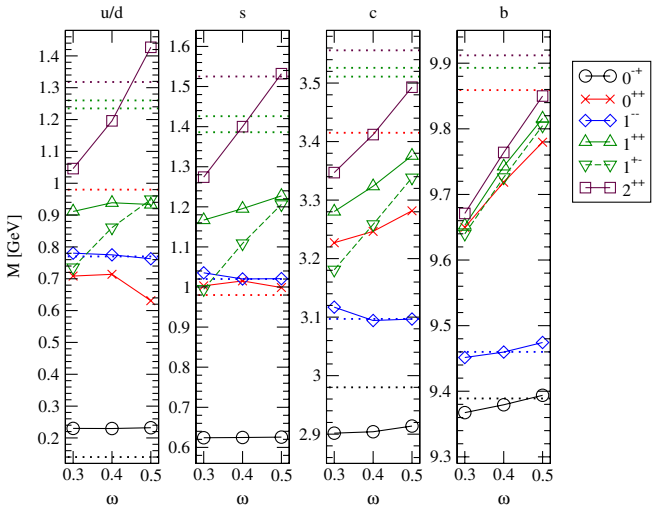

FIG. 2 (color online). Dependence of meson masses on ω. Dotted lines correspond to experimental data [57] where applicable. Figure updated from Ref. [39].

TABLE I. Meson mass of the $s\bar{s}\ 2^{++}$ state with $\omega = 0.4$ GeV with all covariants included as well as with single covariants left out. The change in bound-state mass is given compared to the full result. The results are presented for both the covariants of Eq. (12) and the orthonormal set of covariants constructed thereafter. All numbers are given in GeV.

Covariant missing		None	1	2	3	4	5	6	7	8
Equation (12)	Mass	1.448	1.575	1.455	1.502	1.509	1.502	1.287	1.452	1.450
	Change	+0.000	+0.127	+0.007	+0.054	+0.061	+0.054	−0.161	+0.004	+0.002
Orthonormal	Mass	1.448	1.502	1.445	1.540	1.420	1.669	1.457	1.446	1.508
	Change	+0.000	+0.054	−0.003	+0.092	−0.028	+0.221	+0.009	−0.002	+0.060

noteworthy: First, the 2^{++} mass shows the same ω dependence as the other orbital excitations for each of the four columns. Second, the agreement with experimental data is significantly better than for the often-quoted axial-vector states. In the case of the latter, reconciliation of an RL study constrained by pseudoscalar- and vector-meson observables seems unlikely, while this need apparently not be the case for tensor mesons, indicating that the latter are simpler and not as sensitive to the details of the quark-gluon vertex employed in a DSE-BSE study as the axial-vector states. For our present study, this also *a posteriori* justifies the choice of RL truncation with an effective interaction, which appears to be able to provide a reasonable description of tensor-meson masses, contrary to the expectations.

A further technical note concerns the 2^{++} results for $\omega = 0.5$ GeV: Because of the analytic structure of the quark propagators for this parameter choice, the masses of the 2^{++} mesons are only accessible to us via extrapolation techniques (see the Appendix for a detailed discussion). The uncertainty is always smaller than the size of the symbols in Fig. 2 except for the u/d case, where we get an uncertainty of ± 75 MeV.

In order to elucidate approximation effects or facilitate comparison to other studies, we investigate the effect of leaving out each individual covariant and recompute the mass of the state with the remaining seven. Small differences to the full result then indicate covariants of minor importance. Naturally there is a caveat for such an investigation, namely, that the choice of the covariants is somewhat arbitrary.

In our case we used two sets of covariants: the one given explicitly above in Eq. (12) and the other, orthonormal, constructed according to the principles detailed in Sec. IV. We have performed this test for both sets of covariants and present the results in Table I. We enumerate the orthonormal covariants in the following way: the four terms in (13) multiplied with (17) are numbered 1 to 4, and (13) multiplied with (16) yield covariants 5 to 8. For either set, one needs five of the eight covariants to arrive at a number which is within 1% of the full result. Furthermore, omitting the contribution from $N^{\mu\nu}$ as indicated in [7] for this particular case yields a number which is 7% too low compared to the full result.

VI. CONCLUSIONS AND OUTLOOK

We have reviewed the complete set of Dirac covariants for mesons of spin 2 and the corresponding explicit construction principle for analogous bases for mesons with arbitrary spin J. We have furthermore explored 2^{++} states in a well-established RL truncated model setup of QCD's DSEs and solved the corresponding $q\bar{q}$ BSE numerically for the first time. The results are both reasonable and surprising in that they follow expected patterns, but are closer to experimental data than axial-vector mesons, even in the present simple setup. Our work thus enables an immediate, comprehensive, and fully covariant study of the meson spectrum in a DSE-BSE model setup of QCD. Consequently, the numerical calculation of further states with $J^{PC} = 2^{-+}, 3^{--}$, etc. is work in progress and will be presented in future publications. Naturally, this includes radial excitations of these states and opens up the concrete possibility to investigate Regge trajectories in the covariant DSE-BSE approach.

ACKNOWLEDGMENTS

We would like to acknowledge valuable discussions with R. Alkofer, S. Benić, D. Horvatić, and V. Mader. We are grateful to C.-S. Huang for bringing Ref. [15] to our attention. This work was supported by the Austrian Science Fund *FWF* under Project No. P20496-N16, and was performed in association with and supported in part by the *FWF* doctoral Program No. W1203-N08.

APPENDIX: EXTRAPOLATION TECHNIQUE

As described in Sec. II, the meson BSE, Eq. (1) contains the dressed (anti-)quark propagators $S(q_+)$ and $S(q_-)$, where q_+ and q_- are the (anti-)quark momenta, given by

$$q_+ = q + \eta P =: q + \eta_+ P \tag{A1}$$

$$q_- = q - (1 - \eta)P =: q - \eta_- P. \tag{A2}$$

For a meson with mass M studied in Euclidean momentum space, the total momentum P, taken on shell in the rest frame of the bound state, is purely imaginary, since the on-shell condition implies $P^2 = -M^2$. Together

with the real integration momentum q and the real momentum-partitioning parameters $\eta_\pm$ it is clear that the four-momenta $q_\pm$ and, in particular, also their squares $q_\pm^2$ are complex numbers. It is important to consider the latter, since in our calculations all variables can be defined in terms of scalar products of four-vectors and thus parameterized in terms of the relevant momenta squared, and angle-type variables.

In Fig. 3 we illustrate the typical situation in numerical studies of the coupled quark-DSE–meson-BSE system. As it turns out, the meson mass M (or more generally, the total four-momentum squared P^2) determines the size of the parabolas needed for the sampling of the (anti-)quark propagators as function of their momenta squared. In particular, the parabola is fully defined once M and $\eta_\pm$ are known, as indicated by the filled circle and the filled boxes in the figure. Since the entire interior of the parabola is sampled in the numerical integration in the BSE, singularities inside this domain have to be treated with care. In particular, a fully numerical treatment is nontrivial and has not been realized so far. An important conceptual step in the direction of dealing with singularities in the BSE's integration domain has been taken in [58], where also a more thorough discussion of the problem can be found. If, however, for a given meson mass M singularities appear only outside the domain of integration, e.g., as depicted by the two "X" in Fig. 3, one can use standard numerical integration techniques, as it has been done in the past two decades.

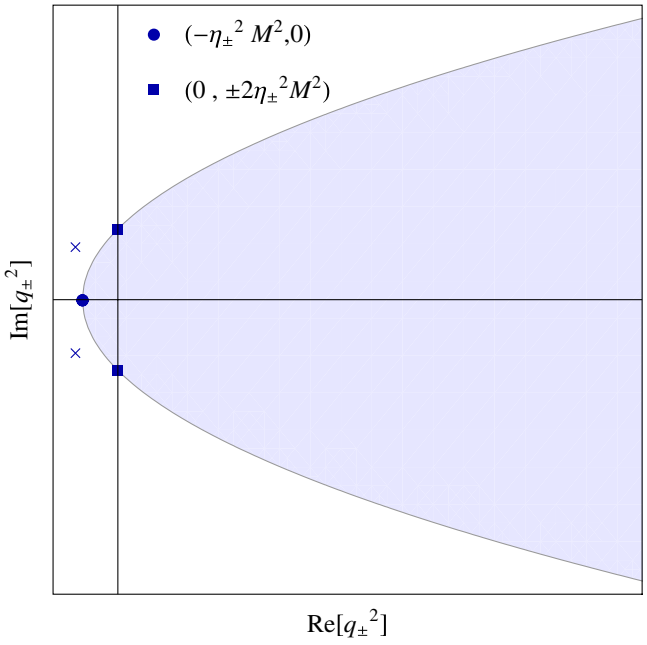

FIG. 3 (color online). The parabola in the complex $q_\pm^2$-plane sampled in the BSE for a meson of mass M together with the typical positions of singularities, marked by "X" (see also the text).

If the meson mass M is expected to lie only a small amount too high for the particular singularity structure of the given (anti-)quark propagators, one can use extrapolation techniques to obtain an estimate for the meson mass from a set of off-shell solutions of the homogeneous BSE. It is important to note here that *a priori* the homogeneous BSE is derived under an on-shell condition; the procedure described here is merely a computational trick to obtain the result. In fact, this strategy is also applied to find the actual on-shell solution, since when solving the homogeneous BSE one has to already know part of the solution, namely, the value of M, in order to numerically solve the equation. The way out of this dilemma is a self-consistency argument, where one introduces an eigenvalue λ in the BSE, Eq. (4), and studies the eigenvalue as a function of the total momentum squared. One obtains

$$\lambda(P^2)\Gamma^{\mu\nu\cdots}(k;P) = \int_q^\Lambda K(k;q;P)S(q_+)\Gamma^{\mu\nu\cdots}(q;P)S(q_-), \tag{A3}$$

and then is able to preset P^2 or M to several different values, and in this way search for that particular value of M where $\lambda(M) = 1$, which restores Eq. (1). In the case where a direct solution is not possible due to singularities in the integration domain, such a procedure leads to a set of data points, which can be extrapolated to $\lambda(M) = 1$. In our case, a reasonable possibility is to use polynomials of degree N

$$\lambda(M) = \sum_{i=0}^{N} a_i M^i, \tag{A4}$$

where for reasons of stability we choose $N = 3, 4, 5$. In Fig. 4 we have plotted the resulting curves for the case with

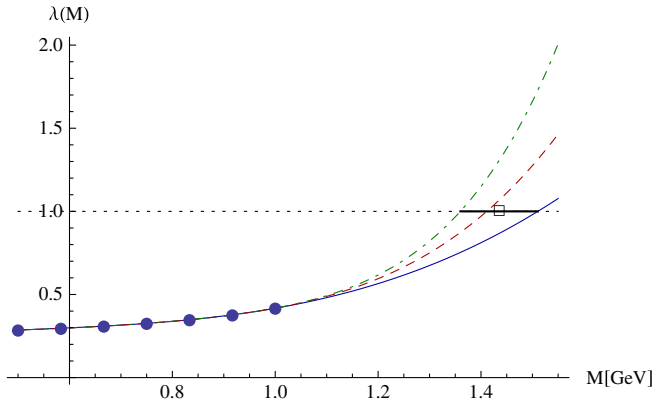

FIG. 4 (color online). Extrapolation of calculated eigenvalues (dots), by polynomials of degree 3 (solid), 4 (dashed), and 5 (dash-dotted), to the value $\lambda(M) = 1$, demarcated by the horizontal dotted line. The central value of the final result (box) and the uncertainty (solid horizontal line) are plotted in the graph as determined (see text).

the largest uncertainty: the dots represent the calculated eigenvalues and the curves show the extrapolations with $N = 3$ (solid line), $N = 4$ (dashed line), and $N = 5$ (dash-dotted line) to the on-shell point $\lambda(M) = 1$, demarcated by the horizontal dotted line. The uncertainty is determined by the largest difference among these three extrapolations and represented by the horizontal solid line on the final result (box).

[1] S. Godfrey and N. Isgur, Phys. Rev. D **32**, 189 (1985).
[2] T. Barnes, S. Godfrey, and E. S. Swanson, Phys. Rev. D **72**, 054026 (2005).
[3] A. Krassnigg, W. Schweiger, and W. H. Klink, Phys. Rev. C **67**, 064003 (2003).
[4] A. Krassnigg, Phys. Rev. C **72**, 028201 (2005).
[5] A. V. Nefediev, J. E. F. T. Ribeiro, and A. P. Szczepaniak, Phys. Rev. D **75**, 036001 (2007).
[6] O. Lakhina and E. S. Swanson, Phys. Lett. B **650**, 159 (2007).
[7] C. H. Llewellyn-Smith, Ann. Phys. (N.Y.) **53**, 521 (1969).
[8] T. Aotsuka and Y. Munakata, Prog. Theor. Phys. **46**, 897 (1971).
[9] M. Fontannaz, Phys. Rev. D **8**, 2640 (1973).
[10] A. N. Mitra and I. Santhanam, Z. Phys. C **8**, 33 (1981).
[11] A. M. Nemirovsky, Phys. Rev. D **28**, 2196 (1983).
[12] Y.-c. Qi and J.-z. Zhang, Nuovo Cimento Soc. Ital. Fis. A **95**, 149 (1986).
[13] K.-I. Aoki, M. Bando, T. Kugo, M. G. Mitchard, and H. Nakatani, Prog. Theor. Phys. **84**, 683 (1990).
[14] K.-I. Aoki, T. Kugo, and M. G. Mitchard, Phys. Lett. B **266**, 467 (1991).
[15] C.-S. Huang, H.-Y. Jin, and Y.-B. Dai, Phys. Rev. D **51**, 2347 (1995).
[16] P. Jain and H. J. Munczek, Phys. Rev. D **48**, 5403 (1993).
[17] P. C. Tiemeijer and J. A. Tjon, Phys. Rev. C **49**, 494 (1994).
[18] M. G. Olsson, S. Veseli, and K. Williams, Phys. Rev. D **53**, 504 (1996).
[19] M. Koll, R. Ricken, D. Merten, B. C. Metsch, and H. R. Petry, Eur. Phys. J. A **9**, 73 (2000).
[20] R. F. Wagenbrunn and L. Y. Glozman, Phys. Rev. D **75**, 036007 (2007).
[21] C. S. Fischer, J. Phys. G **32**, R253 (2006).
[22] C. D. Roberts, M. S. Bhagwat, A. Holl, and S. V. Wright, Eur. Phys. J. Special Topics **140**, 53 (2007).
[23] G. Eichmann, A. Krassnigg, M. Schwinzerl, and R. Alkofer, Ann. Phys. (N.Y.) **323**, 2505 (2008).
[24] D. Nicmorus, G. Eichmann, A. Krassnigg, and R. Alkofer, Phys. Rev. D **80**, 054028 (2009).
[25] G. Eichmann, R. Alkofer, C. S. Fischer, A. Krassnigg, and D. Nicmorus, arXiv:1010.0206.
[26] G. Eichmann, R. Alkofer, A. Krassnigg, and D. Nicmorus, Phys. Rev. Lett. **104**, 201601 (2010).
[27] G. Eichmann, Ph.D.thesis, University of Graz, 2009, arXiv:0909.0703.
[28] R. Alkofer, C. S. Fischer, F. J. Llanes-Estrada, and K. Schwenzer, Ann. Phys. (N.Y.) **324**, 106 (2009).
[29] C. S. Fischer, A. Maas, and J. M. Pawlowski, Ann. Phys. (N.Y.) **324**, 2408 (2009).
[30] T. Maskawa and H. Nakajima, Prog. Theor. Phys. **52**, 1326 (1974).
[31] T. Maskawa and H. Nakajima, Prog. Theor. Phys. **54**, 860 (1975).
[32] T. Kugo and M. G. Mitchard, Phys. Lett. B **282**, 162 (1992).
[33] T. Kugo and M. G. Mitchard, Phys. Lett. B **286**, 355 (1992).
[34] M. Bando, M. Harada, and T. Kugo, Prog. Theor. Phys. **91**, 927 (1994).
[35] H. J. Munczek, Phys. Rev. D **52**, 4736 (1995).
[36] P. Maris, C. D. Roberts, and P. C. Tandy, Phys. Lett. B **420**, 267 (1998).
[37] P. Maris and P. C. Tandy, Phys. Rev. C **61**, 045202 (2000).
[38] P. Maris and P. C. Tandy, Phys. Rev. C **62**, 055204 (2000).
[39] A. Krassnigg, Phys. Rev. D **80**, 114010 (2009).
[40] G. Eichmann, R. Alkofer, I. C. Cloet, A. Krassnigg, and C. D. Roberts, Phys. Rev. C **77**, 042202(R) (2008).
[41] G. Eichmann, I. C. Cloet, R. Alkofer, A. Krassnigg, and C. D. Roberts, Phys. Rev. C **79**, 012202(R) (2009).
[42] R. Williams and C. S. Fischer, arXiv:0912.3711.
[43] L. Chang and C. D. Roberts, arXiv:1003.5006.
[44] P. Maris and C. D. Roberts, Phys. Rev. C **56**, 3369 (1997).
[45] A. Holl, A. Krassnigg, and C. D. Roberts, Phys. Rev. C **70**, 042203(R) (2004).
[46] P. Maris and P. C. Tandy, Phys. Rev. C **60**, 055214 (1999).
[47] A. Krassnigg, Proc. Sci., Confinement 8 (2009).75.
[48] D. Binosi and J. Papavassiliou, Phys. Rep. **479**, 1 (2009).
[49] M. Blank, A. Krassnigg, and A. Maas, Phys. Rev. D **83**, 034020 (2011).
[50] A. Holl, A. Krassnigg, P. Maris, C. D. Roberts, and S. V. Wright, Phys. Rev. C **71**, 065204 (2005).
[51] M. Blank and A. Krassnigg, Comput. Phys. Commun. **182** 1391 (2011).
[52] M. S. Bhagwat, A. Hoell, A. Krassnigg, C. D. Roberts, and S. V. Wright, Few-Body Syst. **40**, 209 (2007).
[53] M. Blank and A. Krassnigg, arXiv:1011.5772.
[54] A. Krassnigg and C. D. Roberts, Nucl. Phys. **A737**, 7 (2004).
[55] C. J. Burden and M. A. Pichowsky, Few-Body Syst. **32**, 119 (2002).
[56] E. M. Corson, *Introduction To Tensors, Spinors, and Relativistic Wave Equations. Relation Structure* (Blackie and Son, London and Glasgow, 1955).
[57] K. Nakamura *et al.* (Particle Data Group), J. Phys. G **37**, 075021 (2010).
[58] M. S. Bhagwat, M. A. Pichowsky, and P. C. Tandy, Phys. Rev. D **67**, 054019 (2003).